J Therm Anal Calorim (2011) 105:279–285
DOI 10.1007/s10973-010-1275-x

Thermal analyses of organic powders made from precipitation polymerization of triallyl monomers

Bharat Indu Chaudhary · Jeffrey M. Cogen · J. Scott Parent

Received: 18 November 2010 / Accepted: 15 December 2010 / Published online: 6 January 2011

Abstract Organic solids have been prepared from radical-initiated activation of solutions composed of tetradecane and triallyl trimesate (TAM) monomer or triallyl phosphate (TAP) monomer using a recently developed variation of precipitation polymerization methods. The powders, which comprise fused aggregates, are shown to be rich in monomer (83–88 wt% TAM or 86–92 wt% TAP), and are believed to be formed by a combination of hydrocarbon addition and allyl group oligomerization. TAM-*g*-tetradecane primary particles are on the order of 500 nm in diameter, while TAP-*g*-tetradecane particles are on the order of 100–200 nm diameter. These products are thermochemically assessed using a combination of differential scanning calorimetry, thermogravimetry and pyrolysis combustion flow calorimetry. The phosphorus-containing TAP-*g*-tetradecane shows exothermic activity around 230 °C, likely due to thermal decomposition of the trialkyl phosphate moiety, and may find use in advanced materials applications.

Keywords Particles · Phosphorus · Triallyl trimesate · Triallyl phosphate

B. I. Chaudhary (✉) · J. M. Cogen
The Dow Chemical Company, 171 River Road, Piscataway, NJ 08854, USA
e-mail: bichaudhary@dow.com

J. Scott Parent
Department of Chemical Engineering, Queen's University, Kingston, ON K7L 3N6, Canada

Introduction

Continued interest in precipitation [1–3] and dispersion [4–6] polymerizations has yielded a range of techniques for preparing crosslinked organic solids with controlled particle size and morphology. These methods typically involve the copolymerization of mono- and di-functional acrylates [7, 8], styrenics [9–11] and their mixtures [12–14] to generate crosslinked spheres with sizes in the micron range. Similar precipitation polymerization processes are used to prepare crosslinked polymer monoliths [15, 16], whose structure porosities are well suited to a wide range of analytical chemistry devices [17, 18].

A variation of precipitation polymerization has recently been described in which intermolecular C–H bond addition from a saturated hydrocarbon (R-H) to an olefin contributes to molecular weight growth [19]. This adaptation broadens the scope of crosslinked particle and monolith syntheses in two ways. In the first place, functional molecules (R-H) that do not contain polymerizable C=C bonds can be incorporated into the product. Secondly, allylic monomers that are not readily homopolymerized can be used to prepare solids in high yield.

This study is concerned with two allylic monomers, triallyl trimesate (TAM) and triallyl phosphate (TAP), whose peroxide-initiated reactions in the presence of tetradecane give novel organic solids. The ability to incorporate TAP is of particular interest, since organophosphorus compounds are known to have application in a variety of advanced materials applications, such as flame retardants [20–31], optoelectronics, mechanics and biology [32, 33]. The precipitation polymerization methods described in this study differ from a conventional copolymerization and polymer grafting approach [34] in that high phosphate concentration can be generated during solids preparation through a simple, high yielding reaction.

The non-volatile TAP-*g*-tetradecane solids described in this report may potentially be useful in advanced materials applications on account of their small size, high ash yields, and ability to serve as a latent source of phosphorus-based acids.

The objective of this study is to evaluate the thermochemical properties of these particles. Thermal analysis was conducted using differential scanning calorimetry (DSC), thermogravimetry (TG) and pyrolysis combustion flow calorimetry (PCFC). DSC can potentially offer insight into the decomposition chemistry, while TG and PCFC provide data about the rate of mass and fuel released by the samples during heating, such data being pertinent to assessment of degradation and flammability [35–37].

Experimental

Materials

Triallyl trimesate (TAM, 99%, Monomer Polymer Inc), triallyl phosphate (TAP, TCI), dicumyl peroxide (DCP, 98%, Sigma-Aldrich) and tetradecane (Sigma-Aldrich) were used as received.

Synthesis of TAM-*g*-tetradecane and TAP-tetradecane

Tetradecane (150 g), DCP (0.9 g, 0.6 wt%) and the desired monomer (TAM or TAP, 7.5 g, 6 wt%) were sealed within a glass pressure tube equipped with a magnetic stir bar and immersed in an oil bath at 170 °C for 25 min. The mixture was cooled to room temperature before isolating the solid product by filtration at reduced pressure. The resulting solids (TAM-*g*-tetradecane and TAP-*g*-tetradecane) were washed with toluene (3 × 20 mL) and dried at reduced pressure.

Instrumentation and analysis

Samples for scanning electron microscopy analysis were sonicated in acetone, deposited on a glass slide by evaporation and gold-sputtered prior to analysis using a JEOL JSM-840 instrument. FT-IR spectra were acquired in transmission mode from KBr pellets using a Thermo Nicolet Nexus 670 spectrometer. Attenuated total reflectance (ATR) spectra were collected using a DuraScope ATR (from Smiths Detection) with DTGS detector and diamond-ZnSe crystal interface. Differential scanning calorimetry (DSC) was conducted with a TA Instruments Q1000 instrument under nitrogen using the following procedure: equilibrate at 30 °C; first heat at 10 °C/min to 150 °C; isothermal for 2 min; cool at 10 °C/min to −60 °C; isothermal for 3 min; second heat at 10 °C/min to 475 °C. Changes in the powder particles were also observed by placing them on a glass substrate, which in turn was placed on a hot plate, and heating up to 340 °C at a rate of approximately 3 °C/s. Thermogravimetry (TG) was conducted in platinum pans with a TA Instruments Model Q5000 under nitrogen or air (at flow rate of 100 cm^3/min) by raising the temperature from 30 to 900 °C at a rate of 10 °C/min. Analyses of TAP-*g*-tetradecane using a ceramic pan gave the same results as obtained using a platinum pan. Pyrolysis Combustion Flow Calorimetry (PCFC), to determine heat release rate as a function of temperature, was conducted using a Micro Combustion Calorimeter Model Govmark MCC-1 in accordance with ASTM D7309-07. Pyrolysis was carried out under nitrogen by heating from 90 to 800 °C at a rate of 1 °C/s. The combustor was run at 900 °C using an oxygen flow rate of 20 cm^3/min and nitrogen flow rate of 80 cm^3/min.

Elemental analysis

The phosphorous content of TAP-*g*-tetradecane was determined using a Perkin-Elmer Optima inductively coupled plasma (ICP) spectrometer, with sample digestion done for 15 min at 240 °C in three parts of sulphuric acid, three parts of nitric acid and one part of perchloric acid. The carbon and hydrogen content of TAP-*g*-tetradecane and TAM-*g*-tetradecane were determined with a Perkin-Elmer 2400 Elemental Analyzer using combustion or pyrolysis to convert the sample elements to simple gases, i.e. CO, CO_2, H_2O, N_2. The oxygen content of TAM-*g*-tetradecane was determined with this instrument, but interference from phosphorous within TAP-*g*-tetradecane prohibited similar determination of its oxygen content. In some cases, an energy dispersive spectrometer (EDS) connected with a FEI Scanning Electron Microscope Quanta 200 was also used to determine proportions of carbon, oxygen and phosphorus in TAP-*g*-tetradecane before and after exposure to elevated temperatures. Unless otherwise mentioned in the text, phosphorus values discussed below are from ICP.

Results and discussion

Precipitation polymerization

Syntheses of the organic monoliths start from clear, homogenous solutions at 170 °C. However, solutions become cloudy within one half-life of the peroxide initiator, and proceed to generate solids which adhere to the side of the reaction vessel. These crosslinked monoliths are completely insoluble in all solvent mixtures, and are

Table 1 Composition of crosslinked monoliths

	Molar elemental composition C:H:O:P	Molar monomer: tetradecane ratio
TAM-*g*-tetradecane	3.7:4.5:1.0:0.0	3.5:1
TAP-*g*-tetradecane	11.2:19.7:4.4:1.0	7.4:1

unaffected by extensive sonication or heating. In theory, the composition of these solids can vary from pure monomer to a 3:1 ratio of tetradecane to TAM/TAP. However, the addition of three tetradecane moieties to the coagent would yield a trialkyl compound with appreciable solubility in non-polar aromatic solvents. Given the insolubility of the products, the monomer-rich compositions listed in Table 1 are not surprising.

Elemental analysis of the TAM-*g*-tetradecane material revealed a composition of 67.8 wt% carbon, 6.8 wt% hydrogen and 24.2 wt% oxygen, which is consistent with a TAM content of 83–88 wt%. Elemental analysis of the TAP-*g*-tetradecane solids revealed that the composition was 52.4 wt% carbon, 7.8 wt% hydrogen and 12.2 wt% phosphorus, which is consistent with a TAP content of 86–92 wt%. The calculated molar monomer:tetradecane ratio for TAM-*g*-tetradecane was 3.5, while that of TAP-*g*-tetradecane was 7.4. It is clear, therefore, that monomer oligomerization is more extensive than hydrocarbon addition, yielding a solid phase that is coagent-rich.

FT-IR analysis of TAM-*g*-tetradecane revealed a strong C=O stretch at 1734 cm^{-1} and a strong C–O stretch at 1238 cm^{-1}, both consistent with large amount of the ester functionality in this solid (Fig. 1). The relatively strong C=C stretch found at 1650 cm^{-1} in triallyl trimesate spectra (not shown) was absent in the spectrum of TAM-*g*-tetradecane, suggesting that little residual allylic C=C functionality existed in the reaction product. TAP-*g*-tetradecane showed a characteristic strong P=O stretch at 1277 cm^{-1} and a characteristic strong P–O stretch at 1020 cm^{-1}, consistent with trialkyl phosphate functionality (Fig. 1). The C=C stretch present at 1651 cm^{-1} in triallyl phosphate (not shown) was relatively weak in the TAP-*g*-tetradecane, again suggesting that allyl group conversion is high. A lack of residual unsaturation in the solids relates not only to reaction efficiency, but also to the potential to further derivatize the material by potential C=C bond activation.

Figure 2a and b provides SEM images of TAM-*g*-tetradecane and TAP-*g*-tetradecane, respectively. Consistent with an earlier report on this variation of precipitation polymerization [19], these solids are composed of primary particles with diameters on the order of 100–500 nm that are fused into larger aggregates. The overall morphology of

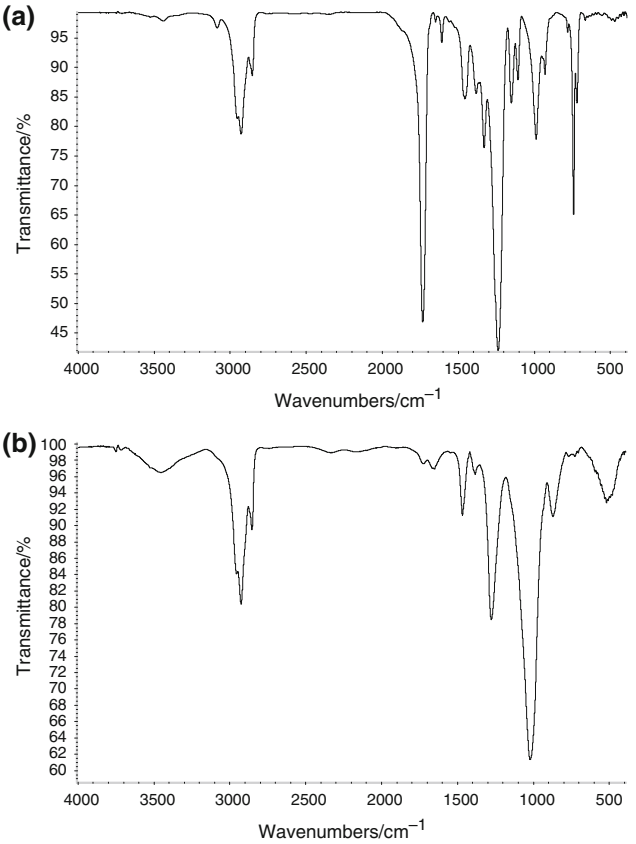

Fig. 1 FTIR spectra of **a** TAM-*g*-tetradecane and **b** TAP-*g*-tetradecane

the TAM-*g*-tetradecane was shown to be that of a high surface area, crosslinked organic monolith [19], and the solubility and microscopy data discussed herein from the TAP-*g*-tetradecane are also consistent with such morphology. Single particles can also be generated by this process, albeit at the expense of solids yield.

Thermal properties

Differential scanning calorimetry (DSC) data acquired from −60 to 150 °C under nitrogen revealed no major phase transitions or thermal decomposition effects for either the TAM or TAP derived solids. Furthermore, the DSC trace for TAM-*g*-tetradecane remained featureless from 150 to 350 °C (Fig. 3), but did show a slight exotherm with peak around 389 °C. In contrast, the DSC trace for TAP-*g*-tetradecane showed a well-defined exotherm (−475 J/g) with a peak heat release rate observed at 230 °C (Fig. 3) and a much smaller exothermic peak around 404 °C. Monomeric trialkylphosphates are known to exhibit exotherms below 300 °C when heated under a nitrogen atmosphere [38]. Although the detailed mechanism leading to those exotherms was not elucidated, the observation of them below 300 °C in the monomeric

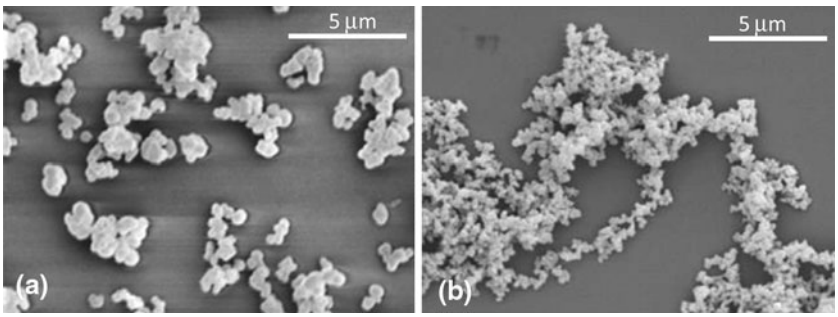

Fig. 2 SEM images of **a** TAM-*g*-tetradecane and **b** TAP-*g*-tetradecane (×6,600)

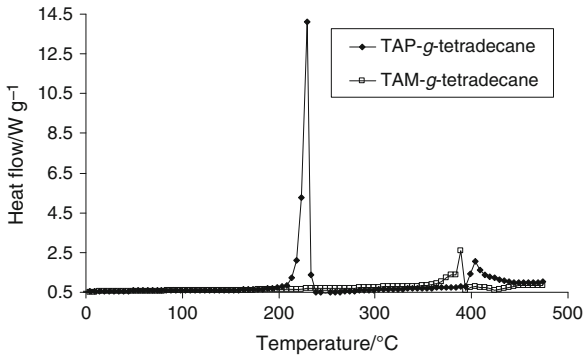

Fig. 3 DSC Analyses of TAP-*g*-tetradecane and TAM-*g*-tetradecane

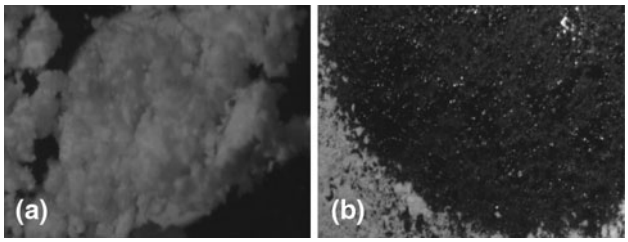

Fig. 4 Thermal decomposition of TAP-*g*-tetradecane at elevated temperature. **a** Room temperature and **b** 240 °C

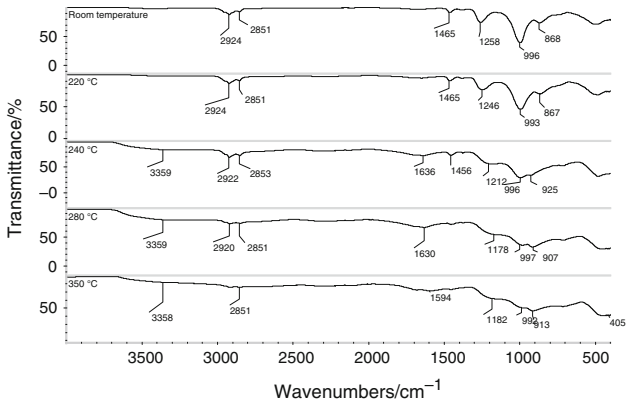

Fig. 5 ATR Spectra of TAP-*g*-tetradecane at different temperatures

analogues is noteworthy in light of the DSC results obtained with the TAP-*g*-tetradecane in this study. It is, therefore, proposed that thermal decomposition of bound phosphate is responsible for the 230 °C exotherm generated by TAP-*g*-tetradecane.

When heated to elevated temperatures on a glass substrate, TAP-*g*-tetradecane was observed to visually decompose, turning black around a temperature of 238 °C (Fig. 4). In contrast, TAM-*g*-tetradecane did not show visual signs of decomposition up to 238 °C. ATR spectra collected on TAP-*g*-tetradecane as a function of temperature are presented in Fig. 5. Many changes in the 600–1400 cm^{-1} region are evident, consistent with changes involving P–O–H, P–O–C, P–O–P, and P=O groups. A peak at a about 3359 cm^{-1} that first appears around 240 °C is consistent with formation of some alcohol groups, while the peak at a about 1630 cm^{-1} that appears prominently in the 240 and 280 °C spectra is consistent with formation of some alkene groups. In the 350 °C spectrum, a peak at 1594 cm^{-1} may include contributions from O=P–OH groups. All these IR data are consistent with elimination of phosphorus-containing species to product phosphorus acids and the alkene, along with some amount of cleavage at P–O to produce some alcohol, possibly via condensation of initially formed P–OH with P–OR to produce P–O–P and R–OH.

The above conclusions are reinforced by the thermogravimetry (TG) results under nitrogen, illustrated in Fig. 6. TAM-*g*-tetradecane showed relatively low weight loss until well above 300 °C, exhibited rapid weight loss when the temperature exceeded 350 °C, and yielded just 4 wt% of the original mass as residue (ash yield). In contrast, TAP-*g*-tetradecane started losing weight around 220 °C, which corresponds to the exotherm observed in DSC (Fig. 3), and resulted in 13 wt% final ash yield. This coincidence of TG and DSC responses in TAP-*g*-tetradecane is attributed to trialkylphosphate decomposition around 220 °C. This low-temperature decomposition produced some non-volatile products, as the rate of mass loss declined after the initial loss around 220 °C, such that the retained weight of TAP-*g*-tetradecane at 420 °C exceeded that recorded for TAM-*g*-tetradecane. Moreover, the final ash generated by TAP-*g*-tetradecane was significantly greater than that of the TAM-derived product.

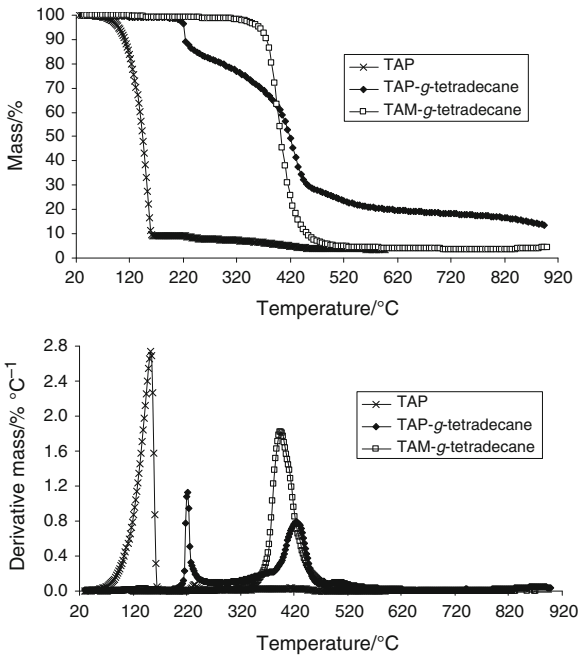

Fig. 6 TG and DTG traces for TAP, TAP-*g*-tetradecane and TAM-*g*-tetradecane under nitrogen

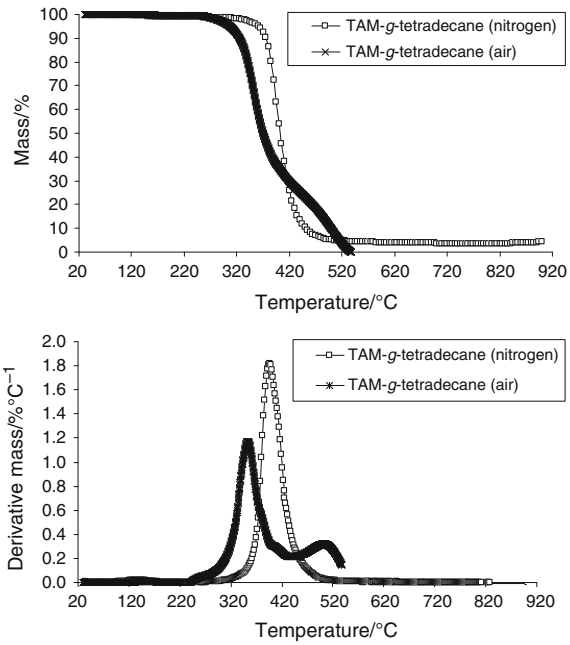

Fig. 7 Effect of environment (nitrogen or air) on TG and DTG traces of TAM-*g*-tetradecane

The effect of environment (nitrogen or air) on the TG performance of both materials was also studied. TAM-*g*-tetradecane decomposed faster in air than in a nitrogen environment, consistent with acceleration of decomposition by oxidative processes (Fig. 7). However, the converse effect was observed with TAP-*g*-tetradecane at temperatures above 300 °C, possibly due to formation of complex char structures that contain oxygen bound to phosphorus, with only slight acceleration in air below this temperature (Fig. 8).

Elemental analysis of the TAP-*g*-tetradecane starting material showed a phosphorus content of 12.2 wt% and a 1:4.3 ratio of phosphorus:carbon. Analysis of a sample that was heated to 360 °C revealed a phosphorus content of 15.0 wt% and a phosphorus:carbon ratio of 1:3.4. Heating TAP-*g*-tetradecane to 900 °C yielded a char that, according to energy dispersive spectrometry (EDS) measurements, contained a phosphorus:carbon ratio which was approximately two times greater than that in the starting material.

Pyrolysis combustion flow calorimetry (PCFC) is a recently developed method for assessing flame retardancy of polymeric materials [36, 37, 39–41]. PCFC measures heat release rate of milligram-sized samples, separately reproducing the solid-state and gas phase processes of flaming combustion in a non-flaming test by rapid controlled pyrolysis of the sample in an inert gas stream followed by high-temperature forced combustion of the pyrolysis gas stream. The rate at which the sample releases its heat of combustion is calculated via oxygen

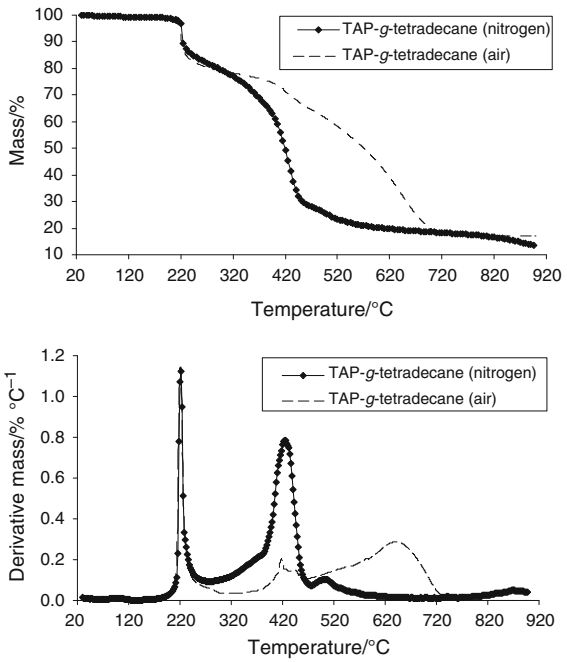

Fig. 8 Effect of environment (nitrogen or air) on TG and DTG traces of TAP-*g*-tetradecane

consumption calorimetry, and the heat of combustion is obtained from the time integral of the heat release rate. Valuable information about the specimen can be obtained from the total amount of heat released as well as the temperature(s) at which peak heat release occurs. The heat release capacity, which is a fundamental material property

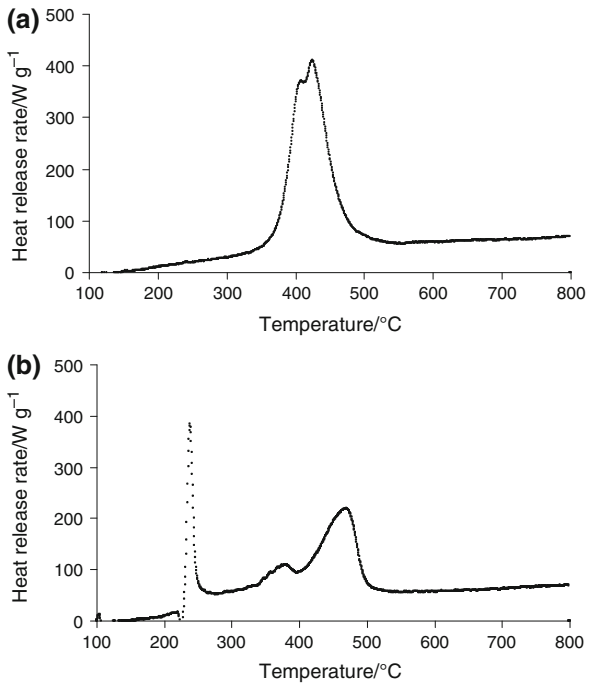

Fig. 9 PCFC analysis of **a** TAM-*g*-tetradecane and **b** TAP-*g*-tetradecane

of pure polymers, is obtained by dividing the peak heat release rate for the sample by the heating rate. Further insight can be gained by measuring the amount of residue remaining in the pyrolyzer after the experiment is completed (ash yield). Thus, PCFC was used to measure total heat released, temperatures of peak heat release rate, heat release capacity, and char yield with the TAM-*g*-tetradecane and TAP-*g*-tetradecane to provide further insight into the thermochemical properties of these materials.

Representative results of PCFC analyses are given in Fig. 9. The peak heat release rate from TAM-tetradecane occurred around 420 °C, close to the decomposition peak temperatures observed by DSC and TG. In contrast, the heat release plot of TAP-tetradecane showed a sharp peak just around 230 °C, which is consistent with the onset of TG decomposition and the exothermic process identified by DSC. Heat release rate maxima were also observed around 380 and 470 °C, corresponding to weight loss rate maxima recorded by TG (Fig. 6). Of particular interest is the 470 °C peak, since it is approximately 50 °C higher than that generated by TAM-*g*-tetradecane. It appears that the 230 °C decomposition of TAP-*g*-tetradecane produces a material structure that is more stable than TAM-*g*-tetradecane, thereby delaying its pyrolysis to higher temperature.

The ash yield, defined here as the weight percent of original mass remaining after PCFC analysis, measured for TAP-*g*-tetradecane was 22% (average of three replicates), considerably greater than the 3% yield recorded for TAM-*g*-tetradecane. However, both materials exhibited comparable heat release capacity (HRC), with TAP-*g*-tetradecane generating 409 ± 77 J/g K and TAM-*g*-tetradecane generating 397 ± 20 J/g K. These results are in the range that some workers have proposed to be indicative of organic materials that possess flame-retardant properties. For example, UL-94 testing of a range of polymers showed that the transition from horizontal burn ratings (slightly flame retardant) to vertical ratings of V2 and higher (greater degree of flame retardancy) occurs below 400 J/g K [36]. UL 94 is a widely used plastics flammability standard from Underwriters Laboratories, which classifies plastics according to how they burn in various orientations and thicknesses. Furthermore, limiting oxygen index testing has shown that the transition to self-extinguishing behaviour in air occurs at heat release capacities below 550 ± 100 J/g K [36]. A transition to self-extinguishing behaviour in the HRC range of 400–600 J/g K has also been reported for wire coatings based on flame-retardant polyolefin formulations [40]. Additional tests would be required to conclusively establish flame-retardant properties of these materials.

Conclusions

TAM-*g*-tetradecane primary particles were on the order of 500 nm in diameter, while TAP-*g*-tetradecane particles were on the order of 100–200 nm. In both cases, elemental analyses indicated that the majority of the particles were derived from the coagent rather than tetradecane: 83–88 wt% in the case of TAM and 86–92 wt% in the case of TAP.

The TAP-based particle exhibited an exotherm in the DSC around 230 °C, which is hypothesized to be from thermal decomposition of the trialkyl phosphate moiety. In TG under nitrogen, the weight loss curves for the two particles crossed over around 395 °C, with the TAP-*g*-tetradecane showing onset of weight loss around 220 °C and higher weight loss at low temperature, but lower weight loss at higher temperature, compared to TAM-*g*-tetradecane. The ratio of phosphorus to carbon in TAP-*g*-tetradecane increased considerably during the course of the TG experiment.

The PCFC heat release profile for TAP-*g*-tetradecane showed a sharp peak around 230 °C and two other peaks below 500 °C, while the TAM-*g*-tetradecane showed a single peak (with a shoulder) below 500 °C.

References

1. Bamford CH, Ledwith A, Sengupta PK. Particulate precipitation polymerization: a convenient procedure for the synthesis of

crosslinked polymers useful as polymeric supports. J Appl Polym Sci. 1980;25:2559–66.
2. Li K, Stover DH. Highly crosslinked micron-range polymer microspheres by dispersion polymerization of divinylbenzene. J Polym Sci A. 1993;31:2473–9.
3. Joso R, Pan EH, Stenzel MH, Davis TP, Barner-Kowollik C, Barner L. Ambient temperature synthesis of well-defined microspheres via precipitation polymerization initiated by UV-irradiation. J Polym Sci A. 2007;45:3482–7.
4. Song JS, Tronc F, Winnik MA. Two-stage dispersion polymerization toward monodisperse, controlled micrometer-sized copolymer particles. J Am Chem Soc. 2004;126:6562–3.
5. Song JS, Winnik MA. Cross-linked, monodisperse, micron-sized polystyrene particles by two-stage dispersion polymerization. Macromolecules. 2005;38:8300–7.
6. ŠponarovÁ D, Horák D. Poly(N, N-diethylacrylamide) microspheres by dispersion polymerization. J Polym Sci A. 2008;46:6263–71.
7. Macková H, Horák D. Effects of the reaction parameters on the properties of thermosensitive poly(N-isopropylacrylamide) microspheres prepared by precipitation and dispersion polymerization. J Polym Sci A. 2006;44:968–82.
8. Dai Z, Yang X, Huang W. Preparation of narrow-disperse or monodisperse poly{[poly(ethylene glycol) methyl ether acrylate]-co-(acrylic acid)} microspheres with ethyleneglycol dimethacrylate as crosslinker by distillation precipitation polymerization. Polym Int. 2007;56:224–30.
9. Downey JS, Frank RS, Li WH, Stöver HDH. Growth mechanism of poly(divinylbenzene) microspheres in precipitation polymerization. Macromolecules. 1999;32:2838–44.
10. Li WH, Stöver HDH. Monodisperse cross-linked core–shell polymer microspheres by precipitation polymerization. Macromolecules. 2000;33:4354–60.
11. Shim SE, Yang S, Choi HH, Choe S. Fully crosslinked poly(-styrene-co-divinylbenzene) microspheres by precipitation polymerization and their superior thermal properties. J Polym Sci A. 2004;42:835–45.
12. Jin JM, Yang S, Sim SE, Choe S. Synthesis of poly(acrylamide-co-divinylbenzene) microspheres by precipitation polymerization. J Polym Sci A. 2005;43:5343–6.
13. Jin JM, Lee JM, Ha MH, Lee K, Choe S. Highly crosslinked poly(glycidyl methacrylate-co-divinyl benzene) particles by precipitation polymerization. Polymer. 2007;48:3107–15.
14. Perrier-Cornet R, Héroguez V, Thienpont A, Babot O, Toupance T. Functional crosslinked polymer particles synthesized by precipitation polymerization for liquid chromatography. J Chromatog A. 2008;1179:2–8.
15. Svec F, Fréchet JMJ. Molded rigid monolithic porous polymers: an inexpensive, efficient, and versatile alternative to beads for the design of materials for numerous applications. Ind Eng Chem Res. 1999;38:34–48.
16. Rohr T, Hilder EF, Donovan JJ, Svec F, Fréchet JMJ. Photografting and the control of surface chemistry in three-dimensional porous polymer monoliths. Macromolecules. 2003;36:1677–84.
17. Gibson GTT, Mugo SM, Oleschuk RD. Surface-mediated effects on porous polymer monolith formation within capillaries. Polymer. 2008;49:3084–90.
18. Svec F, Huber CG. Monolithic materials: promises, challenges, achievements. Anal Chem. 2006;78:2101–7.
19. Wu W, Parent JS, Sengupta SS, Chaudhary BI. Preparation of crosslinked microspheres and porous solids from hydrocarbon solutions: a new variation of precipitation polymerization chemistry. J Polym Sci A. 2009;47:6561–70.
20. Gaan S, Sun G. Effect of phosphorus and nitrogen on flame retardant cellulose: a study of phosphorus compounds. J Anal Appl Pyrol. 2007;78:371–7.
21. Gaan S, Sun G. Effect of phosphorus flame retardants on thermo-oxidative decomposition of cotton. Polym Degrad Stab. 2007;92:968–74.
22. Price D, Pyrah K, Hull TR, Milnes GJ, Ebdon JR, Hunt BJ, Joseph P, Konkel CS. Flame retarding poly(methyl methacrylate) with phosphorus-containing compounds: comparison of an additive with a reactive approach. Polym Degrad Stab. 2001;74:441–7.
23. Lu S, Hamerton I. Recent developments in the chemistry of halogen-free flame retardant polymers. Prog Polym Sci. 2002;27:1661–712.
24. Andersson A, Lundmark S, Maurer FHJ. Evaluation and characterization of ammoniumpolyphosphate–pentaerythritol-based systems for intumescent coatings. J Appl Polym Sci. 2007;104:748–53.
25. Li Q, Jiang P, Su Z, Wei P, Wang G, Tang X. Synergistic effect of phosphorus, nitrogen, and silicon on flame-retardant properties and char yield in polypropylene. J Appl Polym Sci. 2005;96:854–60.
26. Liu YL, Chiu YC. Novel approach to the chemical modification of poly(vinyl alcohol): Phosphorylation. J Polym Sci A. 2003;41:1107–13.
27. Chiang W, Hu HC. Phosphate-containing flame-retardant polymers with good compatibility to polypropylene. I. The effect of phosphate structure on its thermal behavior. J Appl Polym Sci. 2001;81:1125–35.
28. Howell BA, Carter KE. Thermal stability of phosphinated diethyl tartrate. J Therm Anal Calorim. 2010;102:493–8.
29. Vijayakumar CT, Mathan ND, Sarasvathy V, Rajkumar T, Thamaraichelvan A, Ponraju D. Synthesis and thermal properties of spiro phosphorus compounds. J Therm Anal Calorim. 2010;101:281–7.
30. Howell BA, Cho YJ. Thermal decomposition of 2,4,4,5,5-pentaphenyl-1,3,2-dioxaphospholane. J Therm Anal Calorim. 2010;102:517–21.
31. Sarannya V, Sivasamy P, Mathan ND, Rajkumar T, Ponraju D, Vijayakumar CT. Study of thermal properties of intumescent additive pentaerythritol phosphate alcohol. J Therm Anal Calorim. 2010;102:1071–7.
32. Fadhel O, Gras M, Lemaitre N, Deborde V, Hissler M, Geffroy B, Réau R. Tunable organophosphorus dopants for bright white organic light-emitting diodes with simple structures. Adv Mater. 2009;21:1261–5.
33. Judeinstein P, Sanchez C. Hybrid organic–inorganic materials: a land of multidisciplinarity. J Mater Chem. 1996;6:511–25.
34. Mey-Marom A, Behar D. Thermal decomposition studies of cotton radiolytically grafted with phosphorus- and bromine-containing flame retardants. J Appl Polym Sci. 1980;25:691–702.
35. Gracik TD, Long GL. Prediction of thermoplastic flammability by thermogravimetry. Thermochim Acta. 1992;212:163–70.
36. Walters RN, Lyon RE. Molar group contributions to polymer flammability. J Appl Polym Sci. 2003;87:548–63.
37. Lyon RE, Walters RN. Pyrolysis combustion flow calorimetry. J Anal Appl Pyrol. 2004;71:27–46.
38. Shankwalkar SG, Cruz C. Thermal degradation and weight loss characteristics of commercial phosphate esters. Ind Eng Chem Res. 1994;33:740–3.
39. Wilkie CA, Chigwada G, Gilman J, Lyon RE. High-throughput techniques for the evaluation of fire retardancy. J Mater Chem. 2006;16:2023–30.
40. Cogen JM, Lin TS, Lyon RE. Correlations between pyrolysis combustion flow calorimetry and conventional flammability tests with halogen-free flame retardant polyolefin compounds. Fire Mater. 2009;33:33–50.
41. Morgan AB, Wolf JD, Guliants EA, Fernando KAS, Lewis WK. Heat release measurements on micron and nano-scale aluminum powders. Thermochim Acta. 2009;488:1–9.